

# 1 Comparison of drought indicators derived from multiple 2 datasets over Africa

3 **Gustavo Naumann<sup>1</sup>, Emanuel Dutra<sup>2</sup>, Paulo Barbosa<sup>1</sup>, Florian Pappenberger<sup>2</sup>,**  
4 **Fredrik Wetterhall<sup>2</sup> and Jürgen Vogt<sup>1</sup>.**

5 [1]{[European Commission, Joint Research Centre, Ispra, Italy](#)}

6 [2]{European Centre for Medium Range Weather Forecasts, Reading, United Kingdom}

7 Correspondence to: G. Naumann (gustavo.naumann@jrc.ec.europa.eu)

## 8 9 **Abstract**

10 Drought monitoring is a key component to mitigate impacts of droughts. Lack of reliable and  
11 up-to-date [precipitation](#) datasets is a common challenge across the Globe. This study  
12 investigates different datasets and drought indicators on their capability to improve drought  
13 monitoring in Africa. The study was performed for four river basins located in different  
14 climatic regions (the Oum er-Rbia in Morocco, the Blue Nile in Eastern Africa, the Upper  
15 Niger in Western Africa, and the Limpopo in South-Eastern Africa) as well as the Greater  
16 Horn of Africa.

17 The five precipitation datasets compared are the *ECMWF ERA – Interim reanalysis*, the  
18 *Tropical Rainfall Measuring Mission* satellite monthly rainfall product 3B\_43, the *Global*  
19 *Precipitation Climatology Centre* gridded precipitation dataset, the *Global Precipitation*  
20 *Climatology Project* Global Monthly Merged Precipitation Analyses, and the *Climate*  
21 *Prediction Center Merged Analysis of Precipitation*. The set of drought indicators used  
22 includes the Standardized Precipitation Index, the Standardized Precipitation-Evaporation  
23 Index, [Soiland Soil](#) Moisture Anomalies. [Potential Evapotranspiration was also compared](#)  
24 [with the different drought indicators since it's a key process in the water cycle that can](#)  
25 [influence drought conditions.](#)

26 A comparison of the annual cycle and monthly precipitation time series shows a good  
27 agreement in the timing of the rainy seasons. The main differences between the datasets are in  
28 the ability to represent the magnitude of the wet seasons and extremes. Moreover, for the  
29 areas affected by drought, all the drought indicators agree on the time of drought onset and

1 recovery although there is disagreement on the extent of the affected area. In regions with  
2 limited rain gauge data the estimation of the different drought indicators is characterised by a  
3 higher uncertainty. Further comparison suggests that the main source of differences in the  
4 computation of the drought indicators is the uncertainty in the precipitation datasets rather  
5 than the estimation of the distribution parameters of the drought indicators.

6

## 7 **1 Introduction**

8 Assessment of drought impacts requires understanding of regional historical droughts as well  
9 as the [bearingsbehaviours](#) on human activities during their occurrences. Traditional methods  
10 for drought assessment are mainly based on water supply indices derived from precipitation  
11 time-series alone ([Heim 2002](#)). A sparse distribution of rain gauges and short or incomplete  
12 historical rainfall records may, however, lead to significant errors in the estimation of water  
13 supply indices derived from precipitation time-series.

14 As a consequence of drought, many countries in Africa have seen recurrent famines that  
15 affected millions of people (Rojas et al., 2011). Since precipitation is fundamental for rain-fed  
16 crops in these drought-prone regions, improvements in drought monitoring and early warning  
17 will improve our capacity to detect, anticipate, and mitigate famine (Wilhite et al, 2000,  
18 Rowland et al., 2005). However, the lack of reliable and up-to-date climatological data in  
19 many regions of Africa hinders the development of effective real-time drought monitoring  
20 and early warning systems.

21 Recently, several rain gauge and remote sensing based estimations of precipitation became  
22 available, which exhibit discrepancies and limitations in representing rainfall at local and  
23 regional scale. This has been highlighted for daily and monthly precipitation datasets by  
24 Dinku et al (2007; 2008) and Hirpa et al (2010). The authors studied a relatively dense station  
25 network over the Ethiopian highlands and found that at a monthly time scale and a spatial  
26 resolution of 2.5° CMAP and TRMM 3B\_43 performed very well with a bias of less than 10%  
27 and a root mean square error of about 25%. Thiemig et al. (2012; 2013) found that the  
28 Rainfall Estimation Algorithm and TRMM 3B\_42 showed a high potential in reproducing the  
29 interannual variability, the spatial and quantitative distribution and the timing of rainfall  
30 events.

1 Liebmann et al., 2012, studied the spatial variations in the annual cycle comparing GPCP with  
2 TRMM and gauge-based Famine Early Warning System datasets. They found that GPCP  
3 estimates are generally higher than TRMM in the wettest parts of Africa, but the timing of the  
4 annual cycle and onset dates are consistent. Dutra et al., 2013a, found significant differences  
5 (mainly in the equatorial area) in the quality of the precipitation between the ERA-Interim,  
6 GPCP and the Climate Anomaly Monitoring System – Outgoing Longwave Radiation  
7 Precipitation Index (CAMS-OPI) datasets for different river basins in Africa. From these  
8 studies it is evident that the question on which dataset best represents African precipitation is  
9 still not sufficiently answered.

10 The difficulty in establishing a “ground truth” of precipitation in Africa also affects the  
11 uncertainty in the calculation of derivatives of precipitation, like drought indicators, since the  
12 relationship between the quality of a precipitation product and any drought indicator is  
13 nonlinear. This means that errors in the precipitation can be amplified or dampened when a  
14 drought index is computed. Previous works have reviewed and compared several drought  
15 indicators (Heim 2002; Anderson et al 2011, Shukla et al 2011; Vicente-Serrano et al 2012).  
16 However, an agreement between different indicators is not necessarily observed as the  
17 capability to detect droughts changes between indicator, system and region.

18 The main goal of this study was to identify the main sources of uncertainty in the computation  
19 of the drought indicators. Furthermore, an assessment was done on the ability of the different  
20 datasets and drought indicators (SPI, SPEI, PET and SMA) to represent the spatio-temporal  
21 features of droughts in different climate regimes across Africa.

22

## 23 **2 Data and Methods**

### 24 **2.1 Study area**

25 The analysis was performed at continental level over Africa with particular focus on the areas  
26 falling in four river basins (Oum er-Rbia, Limpopo, Niger, and Eastern Nile) as well as the  
27 Greater Horn of Africa (GHA). The regions were defined as the land areas inside each  
28 bounding box (see Figure 1). The area and geographical extent of the study areas are provided  
29 in Table 1. The regional study areas selected cover a range of climates and socio-economic  
30 systems in Africa.

1

## 2 **2.2 Precipitation Data**

3 The five precipitation datasets used were the “ECMWF ERA-INTERIM (ERA-I) Reanalysis”  
4 (approximately  $0.7^{\circ} \times 0.7^{\circ}$ , bilinear interpolation to  $0.5^{\circ} \times 0.5^{\circ}$ ), “Tropical Rainfall Measuring  
5 Mission” (TRMM) satellite monthly rainfall product 3B\_43 ( $0.25^{\circ} \times 0.25^{\circ}$ ), the “Global  
6 Precipitation Climatology Centre” (GPCC) gridded precipitation dataset V.5 ( $0.5^{\circ} \times 0.5^{\circ}$ ), the  
7 Global Precipitation Climatology Project (GPCP) Global Monthly Merged Precipitation  
8 Analyses ( $2.5^{\circ} \times 2.5^{\circ}$ ) and the CPC Merged Analysis of Precipitation (CMAP,  $2.5^{\circ} \times 2.5^{\circ}$ )  
9 (Table 2).

10 This work uses the TRMM Multisatellite Precipitation Analysis –estimation computed at  
11 monthly intervals as TRMM 3B\_43 dataset for the period 1998-2010 (Huffman et al., 2007).  
12 This product combines the estimates generated by the TRMM and other satellite products  
13 (3B-42) with the Climate Anomaly Monitoring System gridded rain gauge data and/or the  
14 GPCC global rain gauge data at  $0.25^{\circ} \times 0.25^{\circ}$  resolution. The GPCC full reanalysis version 5  
15 (Rudolf et al., 1994) was used for 1979 to 2010. This dataset is based on quality-controlled  
16 precipitation observations from a large number of stations (up to 43,000 globally) with  
17 irregular coverage in time.

18 The ECMWF ERA-I reanalysis, the latest global atmospheric reanalysis produced by  
19 ECMWF extends from 1 January 1979 to the present date. See Dee et al. (2011) for detailed  
20 descriptions of the atmospheric model used in ERA-I, the data assimilation system, the  
21 observations used, and various performance aspects. The ERA-I configuration has a spectral  
22 T255 horizontal resolution (about  $0.7^{\circ} \times 0.7^{\circ}$  in the grid-point space) with 60 model vertical  
23 levels. For the present application, the monthly precipitation means were spatially  
24 interpolated (bilinear) to a regular  $0.5^{\circ} \times 0.5^{\circ}$  grid. Three-hourly ERA-I precipitation estimates  
25 are produced by 12 h model integrations starting at 00UTC and 12UTC ~~daily from initial~~  
26 ~~conditions provided by the data assimilation system~~. These short-range forecasts are therefore  
27 mainly constrained by the analysis of upper-air observations of temperature and humidity,  
28 from satellites and in situ instruments.

29 The Global Precipitation Climatology Project (GPCP, Huffman et al., 2009) combines the  
30 precipitation information available from several sources such as the Special Sensor

1 Microwave/Imager (SSM/I) data from the United States Defence Meteorological Satellite  
2 Program satellites, infrared precipitation estimates computed primarily from geostationary  
3 satellites, low-Earth orbit estimates including the Atmospheric Infrared Sounder Television  
4 Infrared Observation Satellite Program (TIROS) Operational Vertical Sounder (TOVS), and  
5 Outgoing Longwave Radiation Precipitation Index data from the NOAA series satellites. The  
6 gauge data included are assembled and analyzed by the Global Precipitation Climatology  
7 Centre (GPCC). The latest version of GPCP v2.2 that was used is available since January  
8 1979 to December 2010 in a regular 2.5°x2.5° grid.

9 The CPC Merged Analysis of Precipitation ("CMAP") is a technique which produces pentad  
10 and monthly analyses of global precipitation in which observations from rain gauges are  
11 merged with precipitation estimates from several satellite-based [algorithms-sensors](#) (infrared  
12 and microwave). The analysis are on a 2.5 x 2.5 degree latitude/longitude grid and extend  
13 back to 1979. For further information refer to Xie and Arkin, (1997).

### 14 **2.3 Drought indicators**

15 The set of hydro-meteorological indicators analysed included the Standardized  
16 Precipitation Index (SPI), Standardized Precipitation-Evaporation Index (SPEI), ~~Potential~~  
17 ~~Evapotranspiration (PET)~~-and Soil Moisture Anomalies (SMA). [A discussion on the possible](#)  
18 [relation of Potential Evapotranspiration \(PET\) with the different indicators is also presented.](#)  
19 [Even if ~~Evaporation~~PET is not a drought indicator itself, it is one of the key processes in the](#)  
20 [water cycle and usually gives a more complete accounting of drought variability and that can](#)  
21 [help to understand differences in drought indicators. However, the estimation of continental](#)  
22 [evapotranspiration fluxes is complex and can be a source of uncertainties when assessing](#)  
23 [drought conditions \(Trambauer et al., 2014\).](#) The SPI was computed with all the datasets  
24 (ERA-I, TRMM, and GPCP) since it only uses precipitation data. The SPEI was computed  
25 with precipitation and potential evapotranspiration from ERA-I, as well as with precipitation  
26 from GPCP and potential evapotranspiration from ERA-I. SMA and PET were directly  
27 obtained from the ERA-I reanalysis. The individual drought episodes from the time series of  
28 all indicators were determined by considering different thresholds of the standardized  
29 indicators. The duration of each dry event was determined as the number of consecutive  
30 months with negative values [of the drought indices](#) (positive for PET) over the period 1998-

1 2010. The monthly drought fractional area was computed for different thresholds but is only  
2 shown for the values below the -1.0 threshold.

### 3 **2.3.1 Standardized Precipitation Index (SPI)**

4 The Standardized Precipitation Index (SPI) was developed by McKee et al. (1993, 1995) to  
5 provide a spatially and temporally invariant measure of the precipitation deficit (or surplus)  
6 for any accumulation timescale (e.g. 3, 6, 12 months). It is computed by fitting a parametric  
7 Cumulative Distribution Function (CDF) to a homogenized precipitation time-series and  
8 applying an equi-probability transformation to the standard normal variable. This gives the  
9 SPI in units of number of standard deviations from the median.

10 Typically, the gamma distribution is the parametric CDF chosen to represent the precipitation  
11 time-series (e.g. McKee et al., 1993, 1995; Lloyd-Hughes and Saunders 2002; Husak et al.,  
12 2007) since it has the advantage of being bounded on the left at zero and positively skewed  
13 (Thom 1958; Wilks 2002). Moreover, Husak et al. (2007) and Naumann et al. (2012) have  
14 shown that the gamma distribution adequately models precipitation time-series in most of the  
15 locations over Africa. In this study we use the Maximum-Likelihood Estimation (MLE)  
16 method to estimate the parameters of the gamma distribution.

17 A persistent negative anomaly of precipitation is the primary driver of drought, resulting in a  
18 successive shortage of water for different natural and human needs. Since SPI values are  
19 given in units of standard deviation from the standardised mean, negative values correspond  
20 to drier periods than normal and positive values correspond to wetter periods than normal.  
21 The magnitude of the departure from the median is a probabilistic measure of the severity of a  
22 wet or dry event.

### 23 **2.3.2 Standardized Precipitation-Evaporation Index (SPEI) and** 24 **Potential Evapotranspiration (PET)**

25 The Standardized Precipitation Evapotranspiration Index (SPEI, Vicente-Serrano et al., 2010)  
26 is based on precipitation and temperature data, and it has the advantage of combining  
27 different time dimensions (like the SPI) with the capacity to include the effects of temperature  
28 variability on drought. The calculation combines a climatic water balance, the accumulation  
29 of a water deficit/surplus at different time scales, and an adjustment to a log-logistic  
30 probability distribution. SPEI is similar to SPI, but it includes the temperature impact via the

1 potential evapotranspiration (PET) that is calculated following Thornthwaite (1948). In the  
2 current work, we used ERA-I 2-meter temperature to derive PET, and the multiscalar index is  
3 calculated as P-PET over the different time-scales and normalized (like the SPI) using the log-  
4 logistic probability distribution.

### 5 2.3.3.2 **Soil Moisture Anomalies (SMA)**

6 Soil moisture anomalies were derived from ERA-I simulations by removing the mean annual  
7 cycle. Further standardization could be achieved by fitting the soil moisture distribution to a  
8 probability distribution (similar to SPI or, SPEI) such as the Beta distribution (Sheffield et al.,  
9 2004) or just a simple z-score (Dutra et al., 2008). In the current work we compare the SMA  
10 z-score following the considerations depicted in Dutra et al., 2008. By normalizing the soil  
11 moisture with the z-score, a classification scheme is obtained that is similar and comparable to  
12 that of McKee et al. (1993) and Vicente Serrano et al. (2012).

## 13 **2.4 Evaluation metrics**

14 The precipitation datasets and drought indicators were assessed using different scores  
15 available in the hydroGOF R-Package (Zambrano-Bigarini, 2013): Spearman's correlation  
16 coefficient (r), Mean Absolute ~~Error~~ Difference (**MAEMAD**), Percent Bias (PBIAS) between  
17 two products and the Index of Agreement (d). Details of the Evaluation scores are listed in the  
18 appendix.

19 A direct quantitative assessment at continental level is difficult due to the lack of an actual  
20 validation dataset that represents the ground truth with adequately high spatial or temporal  
21 resolution. The performance metrics (mean absolute ~~error~~ difference, relative bias and index of  
22 agreement) were used to diagnose the relative reliability of each indicator over different  
23 drought properties. This analysis does not assume that a single dataset or indicator is better  
24 than the other but highlights their temporal and spatial coherency.

25

## 1 **3 Results and discussion**

### 2 **3.1 Comparison of global precipitation datasets**

3 The datasets analysed are based on in-situ data (GPCC), remote sensing estimations (TRMM,  
4 GPCP) and a global circulation model (ERA-I). The datasets are not completely independent.  
5 For example, TRMM and GPCP are mainly based on remote sensing data and GPCP uses  
6 GPCC over land). Figure 2 shows the mean annual precipitation for the ERA-I, GPCC,  
7 GPCP, CMAP and TRMM datasets over Africa. There is an overall agreement between the  
8 datasets with respect to the mean as well as the general spatial patterns of annual  
9 precipitation. These datasets agree on the north-south gradient from the Sahara desert areas in  
10 the North to the tropical savannahs in the Sahel (an area centered at approximately 10°N  
11 spanning from the Atlantic Ocean in the west to the Red Sea in the east). The datasets also  
12 agree in the [areas of maximum](#) precipitation ~~maximum~~ over the African rainforests related to  
13 the location of the Inter-tropical Convergence Zone (ITCZ), as well as -in the drier climate of  
14 the south-western part of Africa. The main differences are observed in the tropical area and  
15 over un-gauged areas. In transition regions from the Sahel to the Sahara TRMM estimations  
16 can exceed GPCC more than twofold while TRMM is substantially lower than the other  
17 estimations along the southwestern coast of West Africa (Liebmann et al., 2012). There is  
18 also a tendency of higher precipitation in the tropical rainforest in GPCP (Liebmann et al.,  
19 2012) and ERA-I (Dutra et al., 2013a, b) compared with the other datasets. ERA-I  
20 overestimates the rainfall in the central African region which is likely to be associated with a  
21 substantial warm bias in the model due to an underestimation of aerosol optical depth in the  
22 region (Dee et al., 2011).

23 For all the datasets and regions analysed the mean annual cycle of precipitation shows good  
24 agreement with respect to the onset and end of the rainy season. This is true even for the GHA  
25 region which is characterized by two rainy seasons (Figure 3). However, with respect to  
26 intensity the results are more heterogeneous. Although in the Limpopo and Oum er-Rbia  
27 basins there is a good agreement between the datasets, for the basins located in the tropical  
28 band the discrepancies are higher with an overestimation of ERA-I in the Eastern Nile Basin  
29 and GHA and an underestimation in the Niger basin.

30 Apparently the density of rain gauges plays a role in determining the agreement between  
31 datasets. The best gauged regions (Oum er-Rbia and Limpopo; Table 1) are those with the



1 lowest dispersion in terms of annual cycle. These two regions (Oum er-Rbia and Limpopo)  
2 are located outside the tropical region, and their precipitation variability is mainly controlled  
3 by large-scale synoptic weather systems, while in the tropical region small-scale convective  
4 events play an important role. In these regions, model uncertainties (for example land-  
5 atmosphere coupling), uncertainties in satellite retrievals as well as poor gauge cover  
6 contribute to the large spread in the mean annual cycles [computed with the different datasets](#).

7 The monthly datasets show a reasonable agreement over all regions in terms of the correlation  
8 coefficients which are usually greater than 0.8 (Table 3). The CMAP dataset deviates with  
9 values below 0.7 in some regions. Oum er-Rbia and Limpopo areas show the best agreement  
10 between datasets with MAE values below 10 mm/month. The bias in those two regions is  
11 below 20 % in all the cases except when TRMM and CMAP are compared (30%).

12 The biggest differences were observed for ERA-I in the Blue Nile and GHA regions. In these  
13 regions the overestimation of monthly precipitation reached 40 mm/month and the bias can  
14 reach 90% in the Blue Nile and around 50% in the GHA. [These discrepancies are mainly due  
15 to the problems of representation of the mean annual cycle of precipitation by atmospheric  
16 models and the lack of in-situ observations \(Mariotti et al., 2011, Dutra et al., 2013b\)](#).

### 17 **3.2 Comparison of drought indicators**

18 The monthly patterns of drought over Africa for January 2000, 2003, 2006 and 2009 show  
19 that dry areas (indicators with negative values) are generally depicted in more than one  
20 indicator, but their consistency varies with the drought characteristics, as well as the spatial  
21 and temporal coverage (Figure 4). Although there is in general a good spatial correspondence  
22 between all the indicators over the study period, there are also areas where there is no  
23 agreement between some indicators, such as in Central Africa between SPI and SPEI.

24 Figure 5 shows the index of agreement (d) between all the drought indicators computed with  
25 ERA-I. Overall, the index of agreement shows that there is a good correspondence between  
26 indicators in all regions with mean d values greater than 0.5 for almost all the comparisons.  
27 PET seems to be uncoupled with the other indicators ~~with showing~~ low values of d. [Maybe  
28 using different PET products could improve the index of agreement, since This may reflect  
29 the high disparities between different PET products that still is observed in the continent have  
30 been reported for Africa \(Trambauer et al., 2014\)](#). However, the effect on the computations of

1 the SPEI is not major, since the agreement of this indicator with the others is still high. Only  
2 the inner Niger Delta is characterized by a weaker agreement, where  $d$  is often below 0.5.

3 Figure 6 shows the evolution of drought areas in 2000, 2003, 2006 and 2009 characterized by  
4 the number of indicators below a certain threshold. In almost all areas there is a good  
5 agreement, with usually more than 3 indicators reporting drought conditions per grid cell.  
6 However, there are some areas with only one indicator below the defined threshold, mostly  
7 over Central Africa. There is scope to take advantage of these discrepancies and agreements  
8 and propose the construction of a composite indicator (Svoboda et al., 2002; Sepulcre-Canto  
9 et al., 2012; Hao and AghaKouchak, 2013). The development of a single composite drought  
10 indicator could improve the detection of the onset of a drought and help to monitor its  
11 evolution more efficiently, at the same time providing information on the uncertainty in the  
12 data. This will allow decision makers and stakeholders to better handle uncertainties in early  
13 warning systems.

14 The individual drought episodes were computed from the time series of all indicators  
15 considering as dry periods all values of standardized indicators below zero. The duration of  
16 each dry event was determined as the number of consecutive months with negative values  
17 (positive for PET) for the period 1998-2010. The average duration of dry episodes lasted  
18 between 2 to 6 months for all indicators, with the largest differences in duration for different  
19 indicators being found in the Niger basin and in the GHA (Figure 7). Overall, dry periods  
20 measured with SPEI tend to be 1 or 2 months more persistent if compared with the other  
21 estimations, while PET is the [indicator-variable](#) with less memory.

22 Figure 8 shows the monthly fractional area under standardised values below -1.0. For the  
23 areas that are under drought, all the datasets agree with the time of onset and recovery but  
24 there are sometimes disagreements on the area affected and this disagreement tends to be  
25 dependent on the threshold selected. In general there is a better agreement if the areas covered  
26 by any standardised indicator below -1.0 are considered. In this analysis the Niger basin and  
27 Greater Horn of Africa present more discrepancies reaching a difference of more than 50%  
28 between SPI and SPEI estimations during the 2009/2010 and 2005/2006 periods respectively.  
29 The soil moisture anomalies tend to define less generalised droughts as it is hard to reach half  
30 the region under dry conditions. However, even if the magnitude of the area is smaller with

1 respect to the other indicators, the soil moisture shows a good correspondence except for the  
2 period 2000/2002 in the inner Niger delta.

3 In order to define how the selected threshold could affect the agreement between datasets a  
4 correlation analysis was performed between different thresholds of SPI and the areas affected  
5 by droughts in each region. Here the results of the different SPI estimations are presented,  
6 however similar results were found for the other indicators (not shown). For almost all  
7 regions (except for Oum er-Rbia where this relationship is almost constant) the correlation  
8 between the different SPI's is higher for thresholds closer to zero (Figure 9). To consider a  
9 higher threshold (i.e. less negative) to define areas affected by drought (e.g. -0.8 or -1),  
10 therefore, will reduce the disagreement between indicators. However it puts a limit to the  
11 detection of the significance and severity of a drought. These results highlight that the main  
12 differences between the indicators appear in the extreme events.

13 Also, the bias between estimations indicates an acceptable departure between estimations  
14 from normal conditions until values near -0.5 (Figure 10). Below this threshold the bias  
15 increases exponentially surpassing quickly a bias of 100% around SPI values of -1. For Niger  
16 and GHA regions there is only a reasonable agreement between ERA-I and GPCP  
17 estimations.

18 Generally in the Oum er-Rbia and Limpopo basins, both extra-tropical regions, the agreement  
19 is high, possibly due to the greater number of in-situ observations and the importance of  
20 large- scale synoptic weather systems in these areas.

21 For the basins located between the tropics a greater disagreement is observed due to different  
22 factors. The main common factor is the remarkable absence of observations to calibrate and  
23 test the datasets. These deficiencies are also more evident in complex mountainous areas such  
24 as the Eastern Nile basin. Furthermore, droughts in equatorial regions are mainly driven by  
25 the absence of convective events during the rainy season. These mesoscale dimension events  
26 are hard to be reproduced by models and even difficult to monitor in areas with scarce in-situ  
27 rain gauges.

28 For drier regions, such as the inner Niger delta and the GHA, the estimation of the distribution  
29 parameters needed for the computation of the standardized indicators can be biased (or lower  
30 bounded) by the large amount of zero or near null precipitation observations. As depicted in  
31 Wu et al. (2007), the estimation of the gamma probability density function and the limited

1 sample size in dry areas reduce the confidence of the SPI values. In these cases, the SPI may  
2 never attain ~~very negative values, failing~~ the necessary threshold and hence failing to detect  
3 some drought occurrences (e.g. SPI always above -1 in Niger and GHA). The discrepancies  
4 between indicators for lower thresholds over regions with limited rain gauge data is  
5 characterised by the uncertainties of extreme values. This suggests that the main sources of  
6 error are the uncertainties in the precipitation datasets that are propagated in the estimation of  
7 the distribution parameters of the drought indicators.

8 The above discussion underlines the fact that drought monitoring and assessment is a difficult  
9 task, not only due to the nature of the phenomenon, but also due to the limitations inherent in  
10 the availability of long-term and high quality datasets for extended regions. The  
11 meteorological datasets as well as the indicators and models used must be selected carefully  
12 and their limitations need to be taken into account. As a consequence no definite conclusion  
13 can be drawn for the use of a single dataset or indicator. Depending on the region to be  
14 studied, different combinations may have to be chosen.

15 Our results further underline the value of maintaining an operational monitoring network at  
16 country, continental or even global level since indirect observations have their intrinsic  
17 uncertainties linked to the availability and reliability of ‘ground truth’ for their calibration.  
18 Without ~~constant proper~~ calibration, model (ERA-I) or algorithm (TRMM)- inherent errors  
19 can propagate ~~up to the same magnitude of the phenomena (or indicator) to be analysed. In~~  
20 ~~fact, the resulting in large drought indicator uncertainties, bringing no added value with~~  
21 ~~respect to using standard climatology. can be so big that for certain events such as droughts~~  
22 ~~with a severity corresponding to an SPI of -2 it is difficult to get an additional value with~~  
23 ~~respect to standard climatologies.~~

24 The development of a combined indicator based on a probabilistic approach (e.g., Dutra et al.,  
25 2013c) could be useful as a monitoring product at continental level ~~in this case~~. However, at  
26 local scale the kind of indicator and the source of data must be chosen carefully taking into  
27 account their limitations.

## 29 **4 Conclusions**

30 This study evaluated the capabilities of different drought indicators, ~~(including SPI, SPEI, and~~  
31 ~~SMA, as well as PET estimations and SMA),~~ in detecting the timing and extension of drought

1 across Africa, using five different precipitation datasets (TRMM, ERA-Interim, GPCC, GPCP  
2 and CMAP). The analysis was performed on a Pan-African scale and on a regional scale  
3 focused on four river basins and on the Greater Horn of Africa.

4 A comparison of the annual cycle and monthly precipitation time series shows a good  
5 agreement in the timing of the peaks, including the Greater Horn of Africa where there are  
6 two rainy seasons. The main differences are observed in the ability to represent the  
7 magnitude of the wet seasons ~~and the extremes~~.

8 The monthly mean precipitation datasets shows good agreement ~~agree~~ over all regions with  
9 the only exception of the CMAP dataset that shows a lower agreement. In the Oum er-Rbia  
10 and Limpopo basins there is a good agreement between the datasets with mean absolute ~~errors~~  
11 differences below 10 mm/month. The bias in those two regions is below 20 %. The worst  
12 performance of ERA-I was observed in the Blue Nile basin, overestimating the monthly  
13 precipitation up to 40 mm/month with a bias of up to 92% with respect to the other datasets ~~of~~  
14 up to 92%. Also in the GHA region the bias is around 50% with an overestimation of up to 17  
15 mm/month.

16 The comparative analysis between TRMM, ERA-I, GPCP and GPCC datasets suggests that it  
17 is feasible to use TRMM time series with high spatial resolution for reliable drought  
18 monitoring over parts of Africa. It is possible to take advantage of this dataset mainly at  
19 regional level due to its high spatial resolution. However, higher discrepancies in SPI  
20 estimations are shown in mountainous areas and areas with a sparse in situ station density.  
21 On the other hand, drought monitoring at continental level with ERA-I performs better  
22 outside the areas influenced by the ITCZ.

23 The comparison between drought indicators suggests that the main discrepancies are due to  
24 the uncertainties in the datasets (driven by a lack of ground information, uncertainties in the  
25 estimation algorithms or the parameterization of the convection) rather than to the estimation  
26 of the distribution parameters. This is why the SPI estimations for the Oum er-Rbia and  
27 Limpopo regions exhibit a better agreement between estimations. While for the other regions  
28 the discrepancies between datasets are in many cases acceptable, greater discrepancies are  
29 observed for the inner Niger Delta when comparing ERA-I estimations with the other  
30 datasets.

1 Regarding the areas that are under drought, all the indicators agree with the time of onset and  
2 recovery but there are sometimes disagreements with respect to the area affected, and the  
3 level of disagreement tends to be dependent on the threshold selected.

4 It is proposed to integrate different indicators and accumulation periods in the form of a  
5 multivariate combined indicator in order to take advantage of their different drought  
6 properties. The probabilistic nature of such an approach would be very helpful for decision  
7 makers and for the combined analysis of multiple risks.

8

### 9 **Acknowledgements**

10 This work was funded by the European Commission Seventh Framework Programme (EU  
11 FP7) in the framework of the Improved Drought Early Warning and Forecasting to Strengthen  
12 Preparedness and Adaptation to Droughts in Africa (DEWFORA) project under Grant  
13 Agreement 265454. Gustavo Naumann thanks Mauricio Zambrano-Bigarini for the important  
14 discussions about different metrics to compare indicators and to make available the  
15 hydroGOF R-package.

16

## 1 Appendix A

2 The Spearman correlation represents the Pearson correlation coefficient computed using the  
3 ranks of the data. Conceptually, the Pearson correlation coefficient is applied to the ranks of  
4 the data rather than to the data values themselves. The Spearman coefficient is a more robust  
5 and resistant alternative to the Pearson product-moment correlation coefficient (Wilks, 2002).  
6 Computation of the Spearman rank correlation can be described as:

$$7 \quad r = 1 - \frac{6 \sum R_i^2}{n(n^2 - 1)} \quad (1)$$

8 where  $R_i$  is the difference in ranks between the  $i$ th pair of data values. In cases of ties, where a  
9 particular data value appears more than once, all of these equal values are assigned their  
10 average rank before computing the  $R_i$ 's.

11 The Mean Absolute ~~Error-Difference~~ (MAD) measures the average magnitude of the ~~errors~~  
12 ~~differences~~ in a set of different estimations of a certain indicator. It measures accuracy for  
13 continuous variables without considering the direction of the error. Also, this quantity is  
14 usually used to measure how close ~~are two datasets or indicators simulated forecasts or~~  
15 ~~predictions (sim)dataset 1 are to the eventual observations (obs)dataset 2~~ as shown in  
16 equation 2

$$17 \quad MAD = \frac{1}{n} \sum_{i=1}^n |X1_i - X2_i| \quad (2)$$

18 ~~where X1 and X are the values of precipitation or drought indicator of dataset 1 and n~~  
19 ~~represents the number of pairs where n represents the number of pairs of the simulated~~  
20 ~~(sim)dataset 1 and observed dataset 2 (obs) indicators.~~

21 The percent bias (PBIAS) measures the average tendency of the ~~simulated~~ values ~~of a certain~~  
22 ~~dataset~~ to be larger or smaller than ~~the a reference observed~~ ones.

$$23 \quad PBIAS = 100 \frac{\sum_{i=1}^n (X1_i - X2_i)}{\sum_{i=1}^n X1_i} \quad (3)$$

24 The optimal value of PBIAS is 0, with low-magnitude values indicating accurate  
25 representation of drought indicators. Positive values indicate an overestimation bias, whereas

1 negative values indicate an underestimation bias. It must be taken into account that this metric  
2 depends on which dataset is considered to represent the observations.

3 The Index of Agreement ( $d$ ) developed by Willmott (1981) as a standardized measure of the  
4 degree of model prediction error varies between 0 and 1. A value of 1 indicates a perfect  
5 match, and 0 indicates no agreement at all (Willmott, 1981). The index of agreement can  
6 detect additive and proportional differences in the observed and simulated means and  
7 variances; however, it is overly sensitive to extreme values due to the squared differences  
8 (Legates and McCabe, 1999).

9 
$$d = 1 - \frac{\sum(x_1 - x_2)^2}{\sum(|x_2 - \bar{x}_1| + |x_1 - \bar{x}_1|)} \quad (4)$$

10



## 1 **References**

- 2 Anderson, M. C., Hain, C., Wardlow, B., Pimstein, A., Mecikalski, J. R., and Kustas, W. P.:  
3 Evaluation of drought indices based on thermal remote sensing of evapotranspiration over the  
4 continental United States. *Journal of Climate*, 24(8), 2025-2044, 2011.
- 5 Dee, D., and Coauthors: The ERA-Interim reanalysis: Configuration and performance of the  
6 data assimilation system. *Quart. J. Roy. Meteor. Soc.*, 137, 553–597, 2011.
- 7 Dinku, T., Ceccato, P., Grover-Kopec, E., Lemma, M., Connor, S. J., and Ropelewski, C. F.:  
8 Validation of satellite rainfall products over East Africa's complex topography. *International*  
9 *Journal of Remote Sensing*, 28(7), 1503-1526, 2007.
- 10 Dinku, T., Chidzambwa, S., Ceccato, P., Connor, S. J., & Ropelewski, C. F.: Validation of  
11 high-resolution satellite rainfall products over complex terrain. *International Journal of*  
12 *Remote Sensing*, 29(14), 4097-4110, 2008.
- 13 Dutra, E., Viterbo, P., and Miranda, P. M. A.: ERA-40 reanalysis hydrological applications in  
14 the characterization of regional drought, *Geophys. Res. Lett.*, 35, L19402,  
15 doi:19410.11029/12008GL035381, 2008.
- 16 Dutra, E., Giuseppe, F. D., Wetterhall, F., & Pappenberger, F.: Seasonal forecasts of droughts  
17 in African basins using the Standardized Precipitation Index. *Hydrology and Earth System*  
18 *Sciences*, 17(6), 2359-2373, 2013a.
- 19 Dutra, E., Magnusson, L., Wetterhall, F., Cloke, H. L., Balsamo, G., Boussetta, S., &  
20 Pappenberger, F.: The 2010–2011 drought in the Horn of Africa in ECMWF reanalysis and  
21 seasonal forecast products. *International Journal of Climatology*, 33, 7, 1720–1729, 2013b.
- 22 Dutra, E., Wetterhall, F., Di Giuseppe, F., Naumann, G., Barbosa, P., Vogt J., Pozzi W., and  
23 Pappenberger F.: Global meteorological drought: Part I - probabilistic monitoring, to be  
24 submitted to HESS, 2013c.
- 25 Hao, Z., & AghaKouchak, A.: Multivariate Standardized Drought Index: A parametric multi-  
26 index model. *Advances in Water Resources*, 57, 12-18, 2013.
- 27 Heim Jr, R. R.: A review of twentieth-century drought indices used in the United States.  
28 *Bulletin of the American Meteorological Society*, 83(8), 1149-1165, 2002.

- 1 Hirpa, F. A., Gebremichael, M., and Hopson, T.: Evaluation of high-resolution satellite  
2 precipitation products over very complex terrain in Ethiopia. *Journal of Applied Meteorology*  
3 *and Climatology*, 49(5), 1044-1051, 2010.
- 4 Huffman and Coauthors: The TRMM Multi-satellite Precipitation Analysis (TMPA): Quasi-  
5 global, multiyear, combined sensor precipitation estimates at fine scales. *J. Hydrometeor.*, 8,  
6 38–55, 2007.
- 7 Huffman, G.J, R.F. Adler, D.T. Bolvin, and Gu G.: Improving the Global Precipitation  
8 Record: GPCP Version 2.1. *Geophys. Res. Lett.*, 36,L17808, doi:10.1029/2009GL040000,  
9 2009.
- 10 Husak, G. J., Michaelsen, J., and Funk, C.: Use of the gamma distribution to represent  
11 monthly rainfall in Africa for drought monitoring applications. *International Journal of*  
12 *Climatology*, 27(7), 935-944, 2007.
- 13 Legates, D. R., and McCabe Jr., G. J.: Evaluating the Use of "Goodness-of-Fit" Measures in  
14 Hydrologic and Hydroclimatic Model Validation, *Water Resour. Res.*, 35(1), 233–241, 1999.
- 15 Liebmann, B., Bladé, I., Kiladis, G. N., Carvalho, L. M., B. Senay, G., Allured, D., Leroux,  
16 S., and Funk, C.: Seasonality of African precipitation from 1996 to 2009. *Journal of Climate*,  
17 25(12), 4304-4322, 2012.
- 18 Lloyd-Hughes, B., and Saunders, M. A.: A drought climatology for Europe. *Int. J. Climatol.*,  
19 22, 1571–1592, 2002.
- 20 [Mariotti, L., Coppola, E., Sylla, M. B., Giorgi, F., and Piani, C.: Regional climate model](#)  
21 [simulation of projected 21st century climate change over an all-Africa domain: Comparison](#)  
22 [analysis of nested and driving model results. \*J. Geophys. Res.\*, 116, D15111,](#)  
23 [doi:10.1029/2010JD015068, 2011.](#)
- 24 McKee T.B., Doesken N.J., and Kleist J.: The Relationship of Drought Frequency and  
25 Duration to Time Scales. *Proc. 8th Conf. on Appl. Clim.*, 17-22 Jan. 1993, Anaheim, CA,  
26 179-184, 1993.
- 27 McKee, T. B., Doesken, N. J., and Kleist, J.: Drought monitoring with multiple time scales.  
28 *Proc. Ninth Conf. on Applied Climatology*, Dallas, TX, Amer. Meteor. Soc. 233-236, 1995.

1 Naumann, G., Barbosa, P., Carrao, H., Singleton, A., and Vogt, J.: Monitoring Drought  
2 Conditions and Their Uncertainties in Africa Using TRMM Data. *Journal of Applied*  
3 *Meteorology and Climatology*, 51(10), 1867-1874, 2012.

4 Rojas, O., Vrieling, A., and Rembold, F.: Assessing drought probability for agricultural areas  
5 in Africa with coarse resolution remote sensing imagery. *Remote Sensing of Environment*  
6 115.2, 343-352, 2011.

7 Rowland, J., Verdin, J., Adoum, A., and Senay, G.: Drought monitoring techniques for famine  
8 early warning systems in Africa, in: *Monitoring and Predicting Agricultural Drought: A*  
9 *Global Study*, edited by: Boken, V. K., Cracknell, A. P., and Heathcote, R. L., Oxford  
10 University Press, New York, 252–265, 2005.

11 Rudolf, B., W. Rueth, and Schneider, U.: Terrestrial precipitation analysis: Operational  
12 method and required density of point measurements. *Global Precipitation and Climate*  
13 *Change*, M. Desbois and F. Desahmond, Eds., Springer-Verlag, 173–186, 1994.

14 Sepulcre-Canto, G., Horion, S., Singleton, A., Carrao, H., and Vogt, J.: Development of a  
15 Combined Drought Indicator to detect agricultural drought in Europe. *Natural Hazards and*  
16 *Earth System Science*, 12(11), 3519-3531, 2013.

17 Sheffield, J., Goteti, G., Wen, F. H., and Wood, E. F.: A simulated soil moisture based  
18 drought analysis for the United States, *J. Geophys. Res.*, 109(D24), 2004.

19 Shukla, S., Steinemann, A. C., & Lettenmaier, D. P.: Drought monitoring for Washington  
20 State: Indicators and applications. *Journal of Hydrometeorology*, 12(1), 66-83, 2011.

21 Svoboda, M. D., and Coauthors: The drought monitor. *Bull. Amer. Meteor. Soc.*, 83, 1181-  
22 1189, 2002.

23 Thiemig, V., Rojas, R., Zambrano-Bigiarini, M., Levizzani, V., and De Roo, A.: Validation of  
24 Satellite-Based Precipitation Products over Sparsely Gauged African River Basins. *Journal of*  
25 *Hydrometeorology*, 13(6), 1760-1783, 2012.

26 Thiemig, V., Rojas, R., Zambrano-Bigiarini, M., and De Roo, A.: Hydrological Evaluation of  
27 Satellite-Based Rainfall Estimates over the Volta and Baro-Akobo Basin. *Journal of*  
28 *Hydrology*, 499, 324-338, 2013.

29 Thom, H. C.: A note on the gamma distribution. *Monthly Weather Review*, 86(4), 117-122,  
30 1958.

1 Thornthwaite, C. W.: An approach toward a rational classification of climate. *Geogr. Rev.*,  
2 38, 55–94, 1948.

3 [Trambauer, P., Dutra, E., Maskey, S., Werner, M., Pappenberger, F., van Beek, L. P. H., and](#)  
4 [Uhlenbrook, S.: Comparison of different evaporation estimates over the African continent,](#)  
5 [Hydrol. Earth Syst. Sci., 18, 193-212, doi:10.5194/hess-18-193-2014, 2014.](#)

6 Vicente-Serrano, S. M., Beguería, S., and López-Moreno, J. I.: A multiscalar drought index  
7 sensitive to global warming: the standardized precipitation evapotranspiration index. *Journal*  
8 *of Climate*, 23(7), 1696-1718, 2010.

9 Vicente-Serrano, S. M., Beguería, S., Gimeno, L., Eklundh, L., Giuliani, G., Weston, D., El  
10 Kenawy, A., López-Moreno, J., Nieto, R., Ayenew T., Konte, D., Ardö, J., and Pegram, G.  
11 G.: Challenges for drought mitigation in Africa: The potential use of geospatial data and  
12 drought information systems. *Applied Geography*, 34, 471-486, 2012.

13 Wilhite, D. A., and Svoboda, M., D.: "Drought early warning systems in the context of  
14 drought preparedness and mitigation." *Early warning systems for drought preparedness and*  
15 *drought management*, 1-21, 2000.

16 Wilks D.S.: *Statistical Methods in the Atmospheric Sciences*. Elsevier Academic Press  
17 Publications, 467 pp., 2002.

18 Willmott, C. J.: On the validation of models. *Physical Geography*, 2, 184–194, 1981.

19 Wu, H., Svoboda, M. D., Hayes, M. J., Wilhite, D. A., and Wen, F.: Appropriate application  
20 of the standardized precipitation index in arid locations and dry seasons. *International Journal*  
21 *of Climatology*, 27(1), 65-79, 2007.

22 Xie, P., and Arkin, P. A.: Global precipitation: A 17-year monthly analysis based on gauge  
23 observations, satellite estimates, and numerical model outputs. *Bull. Amer. Meteor. Soc.*, 78,  
24 2539 – 2558, 1997.

25 Zambrano-Bigiarini M.: hydroGOF: Goodness-of-fit functions for comparison of simulated  
26 and observed hydrological time series. R package version 0.3-7. [http://CRAN.R-](http://CRAN.R-project.org/package=hydroGOF)  
27 [project.org/package=hydroGOF](http://CRAN.R-project.org/package=hydroGOF), 2013.

28

29

1

2 Table 1. Geographical extent of the African regions and number of grid cells analysed for  
3 each dataset. For GPCC, the percentage of stations per grid and the percentage of pixels  
4 without stations are respectively shown between brackets.

<b>Region</b>	<b>Area (10<sup>6</sup>xKm<sup>2</sup>)</b>	<b>Longitude-Latitude</b>	<b>GPCC Grid cells</b>
A - Oum er-Rbia	0.49	[10°W-0°E]X[31°N-35°N]	36 (52, 65)
B - Niger	1.48	[10°W-0°E]X[6°N-18°N]	120 (23, 70)
C - Eastern Nile	1.23	[30°E-40°E]X[7°N-17°N]	100 (23, 75)
D -Limpopo	0.94	[25°E-34°E]X[26°S-20°S]	54 (56, 44)
E -GHA	2.22	[40°E-52°E]X[2°S-12°N]	180 (15, 85)

5

6

7

8

1 Table 2. Description of global datasets available in near-real time that could be used for  
 2 monitoring precipitation conditions at continental level.

<i>Datasets</i>	<i>resolution</i>	<i>period</i>	<i>Source</i>	<i>Update</i>
<b>ERA INTERIM</b>	0.5°x0.5°	1979-present	ECMWF Reanalysis	½ month
<b>TRMM 3B-43 v.6</b>	0.25°x0.25	1998-present	Remote Sensing Estimate (combination 3B-42, CAMS and/or GPCC)	1 or 2 months
<b>GPCC v.5</b> <del>(Combined)</del>	0.5°x0.5° <del>(1°x1°)</del>	1901-2010 <del>(-present)</del>	In-situ data	1 month
<b>GPCP v.2.2</b>	2.5°x2.5°	1979-2010	Remote Sensing Estimate(merged from microwave, infrared and sounder data and precipitation gauge analyses (GPCC).	irregular
<b>CMAP</b>	2.5°x2.5°	1979-2009	Remote Sensing Estimate (GPI, OPI,S SM/I scattering, SSM/I emission and MSU + NCEP/NCAR Reanalysis )	irregular

3  
 4  
 5

1 Table 3. Correlation coefficient (r), Mean absolute ~~error-difference~~ (MAEMAD) and percent  
 2 bias (%) between the different precipitation datasets averaged over each region for the  
 3 common period 1998-2010. All correlations are significant at 99%.

		<i>TRMM</i>			<i>GPCC</i>			<i>GPCP</i>			<i>CMAP</i>			<i>ERA-I</i>		
		r	MAD	BIAS	r	MAD	BIAS	r	MAD	BIAS	r	MAD	BIAS	r	MAD	BIAS
<b>OER</b>	<b>TRMM</b>	-	-	-	0.99	2.5	2.7	0.99	2.9	6.7	0.74	7.8	42.8	0.95	7.3	26.3
	<b>GPCC</b>	0.99	2.5	-2.6	-	-	-	0.99	2.5	4.2	0.94	4.7	23.1	0.95	6.7	24.4
	<b>GPCP</b>	0.99	2.9	-6.2	0.99	2.5	-4	-	-	-	0.73	6.5	33.9	0.95	5.7	18.4
	<b>CMAP</b>	0.74	7.8	-30	0.94	4.6	-18.7	0.73	6.5	-25.3	-	-	-	0.68	7.0	-11.6
	<b>ERA-I</b>	0.95	7.3	-20.8	0.95	6.6	-19.6	0.95	5.7	-15.5	0.68	7.0	13.1	-	-	-
<b>NIG</b>	<b>TRMM</b>	-	-	-	0.99	5.8	-1.9	0.98	13.6	-14.5	0.8	13.9	7.2	0.94	23.2	8
	<b>GPCC</b>	0.99	5.8	1.9	-	-	-	0.99	11.6	-14.1	0.97	6.9	-1	0.95	22.2	8.3
	<b>GPCP</b>	0.98	13.6	17	0.99	11.5	16.4	-	-	-	0.82	16.7	25.4	0.95	25.8	26.4
	<b>CMAP</b>	0.8	13.8	-6.7	0.97	6.9	1	0.82	16.8	-20.3	-	-	-	0.78	25.8	0.7
	<b>ERA-I</b>	0.94	23.1	-7.4	0.95	22.2	-7.7	0.95	25.8	-20.9	0.78	25.8	-0.7	-	-	-
<b>ENL</b>	<b>TRMM</b>	-	-	-	0.94	17.6	-23.7	0.93	17.4	-22.4	0.82	15.3	-0.6	0.93	43.9	-48.1
	<b>GPCC</b>	0.94	17.6	31	-	-	-	1	2.7	1.9	0.97	12.1	22.5	0.97	29.9	-32.3
	<b>GPCP</b>	0.93	17.4	28.9	1	2.66	-1.9	-	-	-	0.85	14.3	28.2	0.97	30.1	-33.1
	<b>CMAP</b>	0.82	15.3	0.6	0.97	12.1	-18.4	0.85	14.3	-22	-	-	-	0.86	43.4	-47.8
	<b>ERA-I</b>	0.93	43.9	92.8	0.97	29.9	47.6	0.97	30.1	49.5	0.86	43.4	91.7	-	-	-
<b>LIM</b>	<b>TRMM</b>	-	-	-	0.98	7.03	8.9	0.97	8.4	6.7	0.76	12.6	20.6	0.96	10.4	9
	<b>GPCC</b>	0.98	7.0	-8.2	-	-	-	0.99	5.1	-3.3	0.91	8.3	1.8	0.98	8.1	-1.5
	<b>GPCP</b>	0.97	8.4	-6.3	0.99	5.1	3.4	-	-	-	0.79	9.9	13	0.97	8.8	2.1
	<b>CMAP</b>	0.76	12.6	-17	0.91	8.3	-1.8	0.79	9.9	-11.5	-	-	-	0.79	12.8	-9.6
	<b>ERA-I</b>	0.96	10.4	-8.2	0.98	8.1	1.5	0.97	8.8	-2.1	0.79	12.8	10.6	-	-	-
<b>GHA</b>	<b>TRMM</b>	-	-	-	0.82	9.8	-4.2	0.88	6.6	1.7	0.72	9.2	11.2	0.84	17.8	-34
	<b>GPCC</b>	0.82	9.8	4.4	-	-	-	0.9	8.2	7.1	0.84	9.4	8.4	0.83	17.1	-30.9
	<b>GPCP</b>	0.88	6.6	-1.7	0.9	8.2	-6.6	-	-	-	0.7	9.6	9.3	0.92	16.4	-35.1
	<b>CMAP</b>	0.72	9.2	-10.1	0.84	9.4	-7.8	0.7	9.6	-8.5	-	-	-	0.61	22.7	-40.6
	<b>ERA-I</b>	0.84	17.8	51.5	0.83	17.1	44.7	0.92	16.4	54.1	0.61	22.7	68.4	-	-	-

4  
5  
6  
7  
8  
9  
10

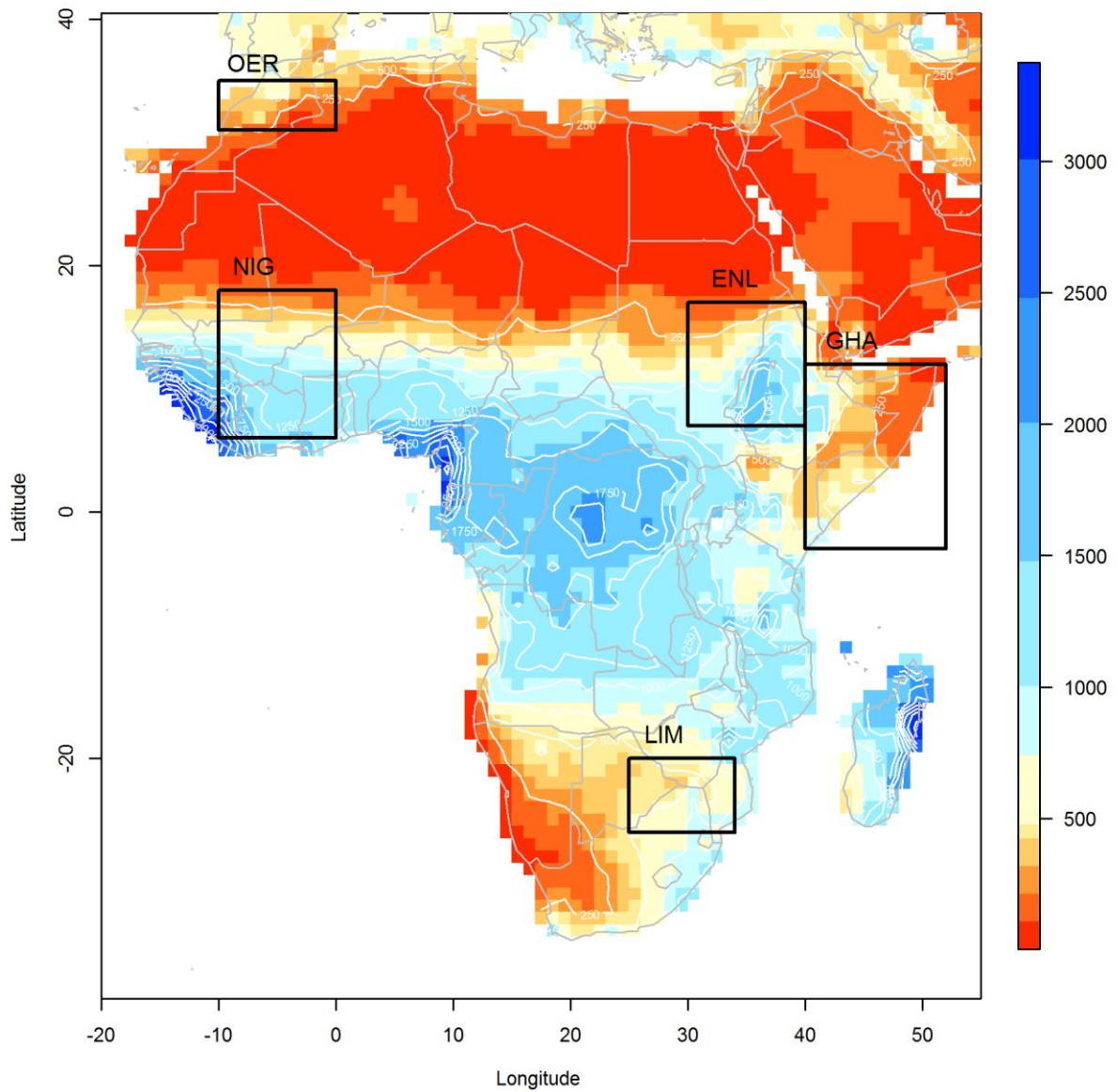
1 Table 4. Spearman correlation coefficient (r), mean absolute ~~error~~ difference (MAEMAD)  
 2 between the different SPI-3 estimations averaged over each region for the common period  
 3 1998-2010

		<i>TRMM</i>		<i>GPCC</i>		<i>GPCP</i>		<i>ERA-I</i>	
		<i>r</i>	<i>MAD</i>	<i>r</i>	<i>MAD</i>	<i>r</i>	<i>MAD</i>	<i>r</i>	<i>MAD</i>
<b>Oumer-Rbia</b>	<b>TRMM</b>	-	-	0.89	0.28	0.81	0.38	0.84	0.37
	<b>GPCC</b>	0.89	0.28	-	-	0.81	0.35	0.81	0.34
	<b>GPCP</b>	0.81	0.38	0.81	0.35	-	-	0.74	0.5
	<b>ERA-I</b>	0.84	0.37	0.81	0.34	0.74	0.5	-	-
<b>Niger</b>	<b>TRMM</b>	-	-	0.85	0.26	0.79	0.38	0.71	0.5
	<b>GPCC</b>	0.85	0.26	-	-	0.91	0.29	0.72	0.46
	<b>GPCP</b>	0.79	0.38	0.91	0.29	-	-	0.67	0.65
	<b>ERA-I</b>	0.71	0.5	0.72	0.46	0.67	0.65	-	-
<b>Blue Nile</b>	<b>TRMM</b>	-	-	0.54	0.54	0.53	0.55	0.6	0.5
	<b>GPCC</b>	0.54	0.54	-	-	0.92	0.27	0.57	0.41
	<b>GPCP</b>	0.53	0.55	0.92	0.27	-	-	0.67	0.46
	<b>ERA-I</b>	0.6	0.5	0.57	0.41	0.67	0.46	-	-
<b>Limpopo</b>	<b>TRMM</b>	-	-	0.91	0.28	0.84	0.39	0.8	0.46
	<b>GPCC</b>	0.91	0.28	-	-	0.92	0.27	0.91	0.33
	<b>GPCP</b>	0.84	0.39	0.92	0.27	-	-	0.88	0.35
	<b>ERA-I</b>	0.8	0.46	0.91	0.33	0.88	0.35	-	-
<b>GHA</b>	<b>TRMM</b>	-	-	0.58	0.4	0.65	0.44	0.61	0.44
	<b>GPCC</b>	0.58	0.4	-	-	0.86	0.29	0.58	0.42
	<b>GPCP</b>	0.65	0.44	0.86	0.29	-	-	0.68	0.45
	<b>ERA-I</b>	0.61	0.44	0.58	0.42	0.68	0.45	-	-

4  
5  
6  
7  
8  
9  
10  
11  
12



1



2

3 Figure 1. Annual mean precipitation from the GPCP dataset and African regions used in this  
4 analysis as defined in Table 1. (OER: Oum er-Rbia; NIG: Inner Niger Delta; ENL: Eastern  
5 Nile, LIM: Limpopo basin and GHA: Greater Horn of Africa.

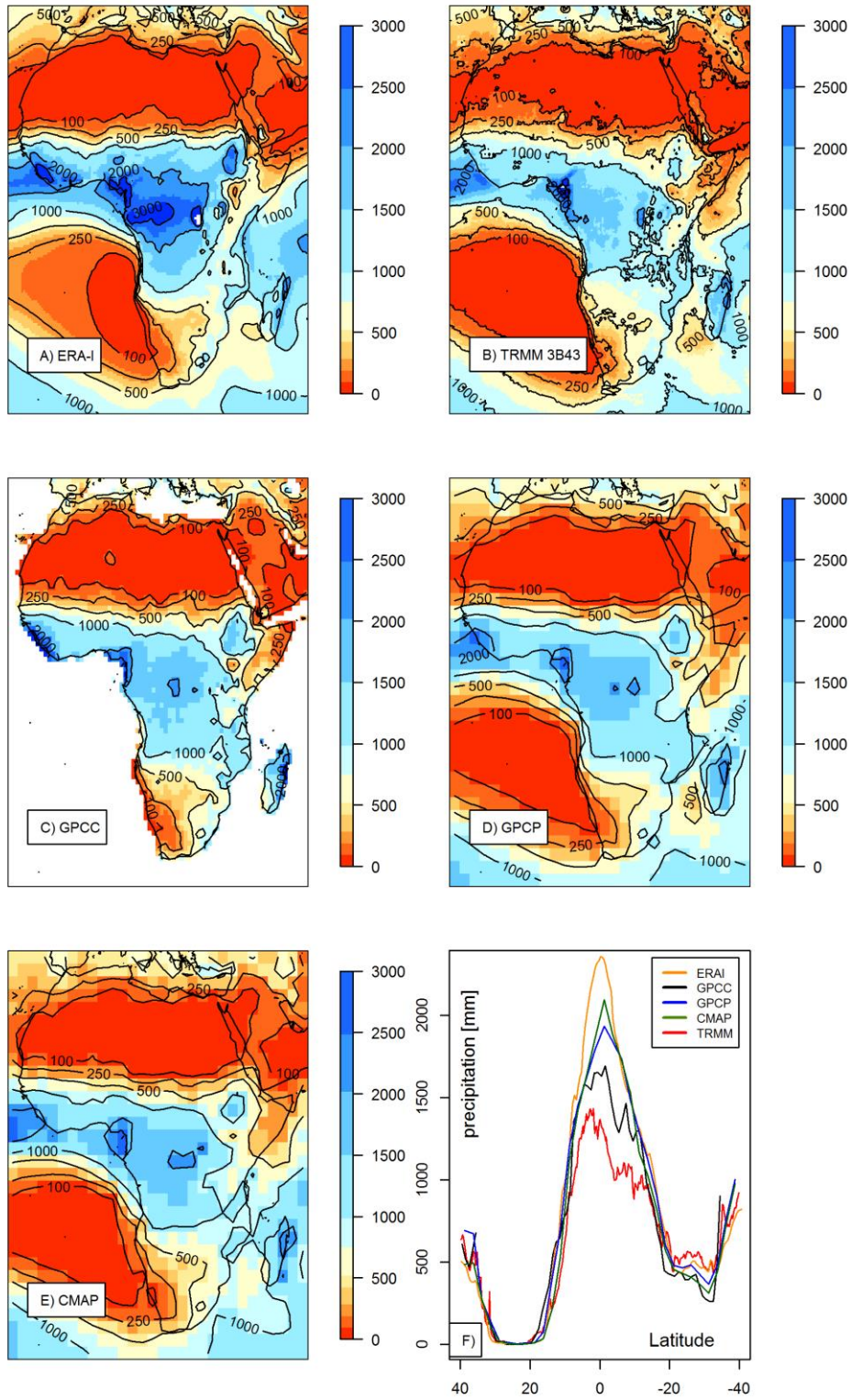
6

7

8

9

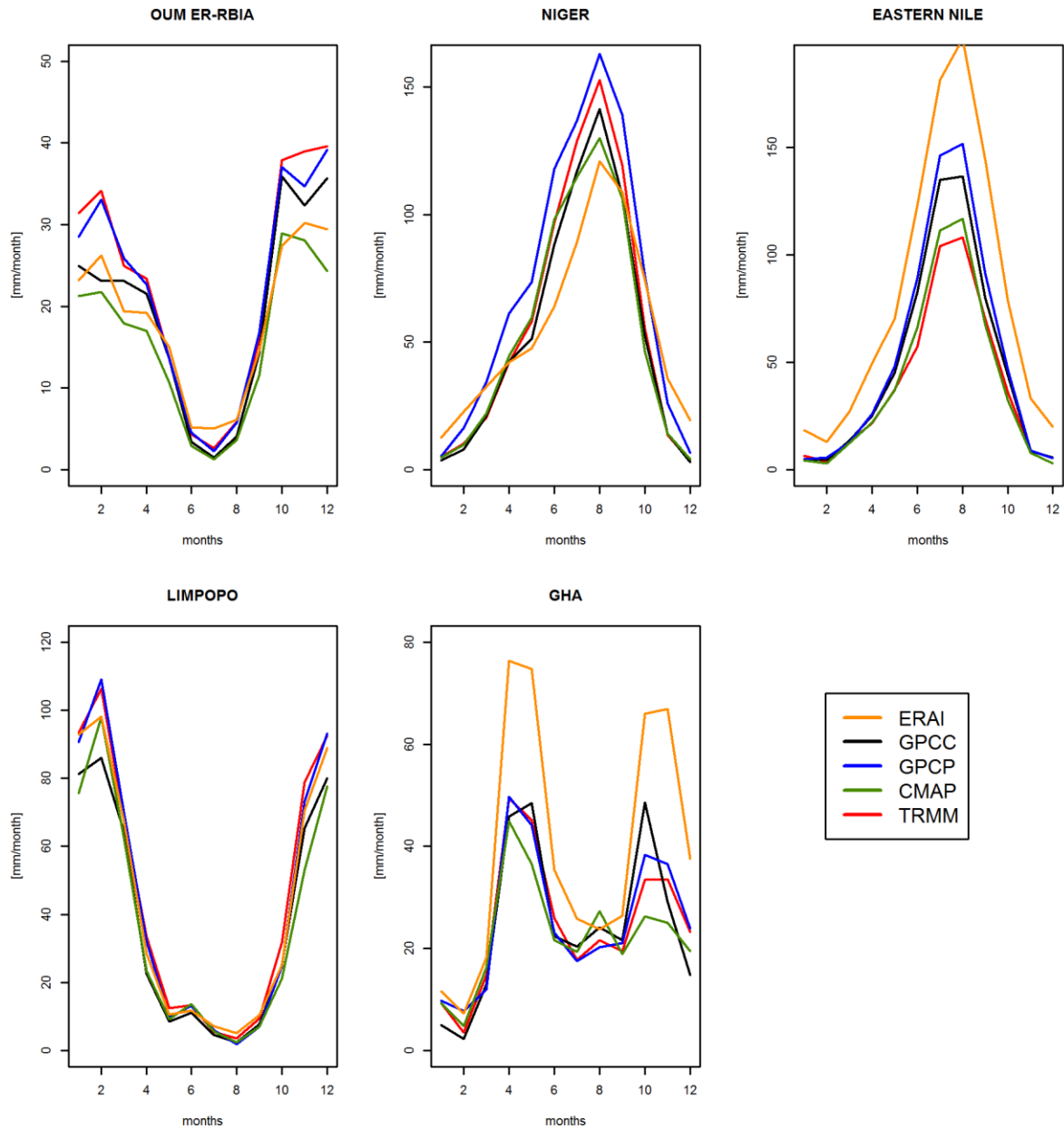
1



2

3 Figure 2. A-E) Mean annual precipitation (mm/year) from different datasets for the common  
4 period 1998-2010, F) longitudinal cross section at 25°E of mean annual precipitation.

5



1

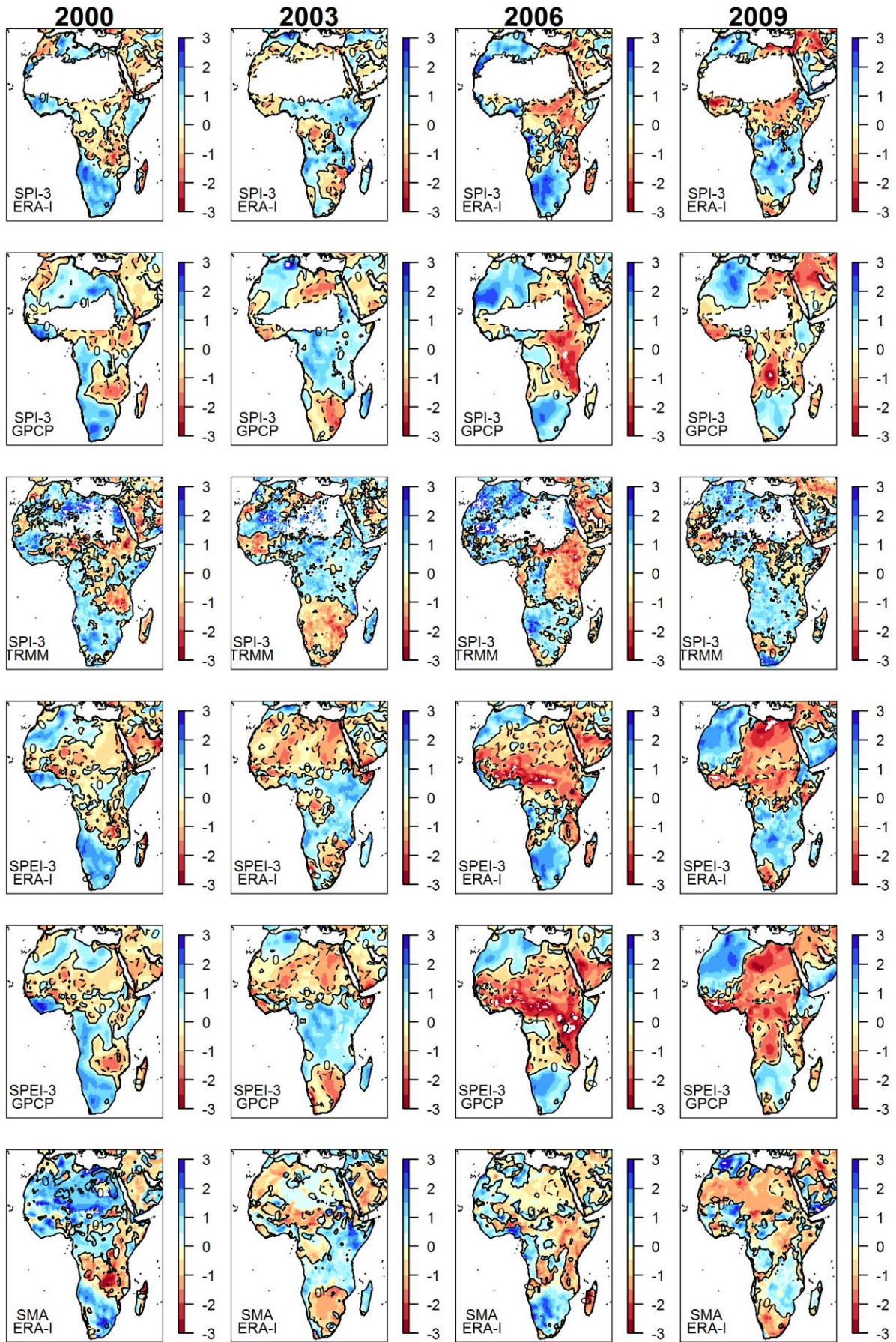
2 Figure 3. Mean annual cycle of precipitation from the different datasets averaged over the five  
 3 regions defined in Figure 1 (OER: Oum er-Rbia, NIG: Inner Niger Delta, NIL: Eastern Nile,  
 4 LIM: Limpopo basin and GHA: Greater Horn of Africa) for the common period 1998-2010.

5

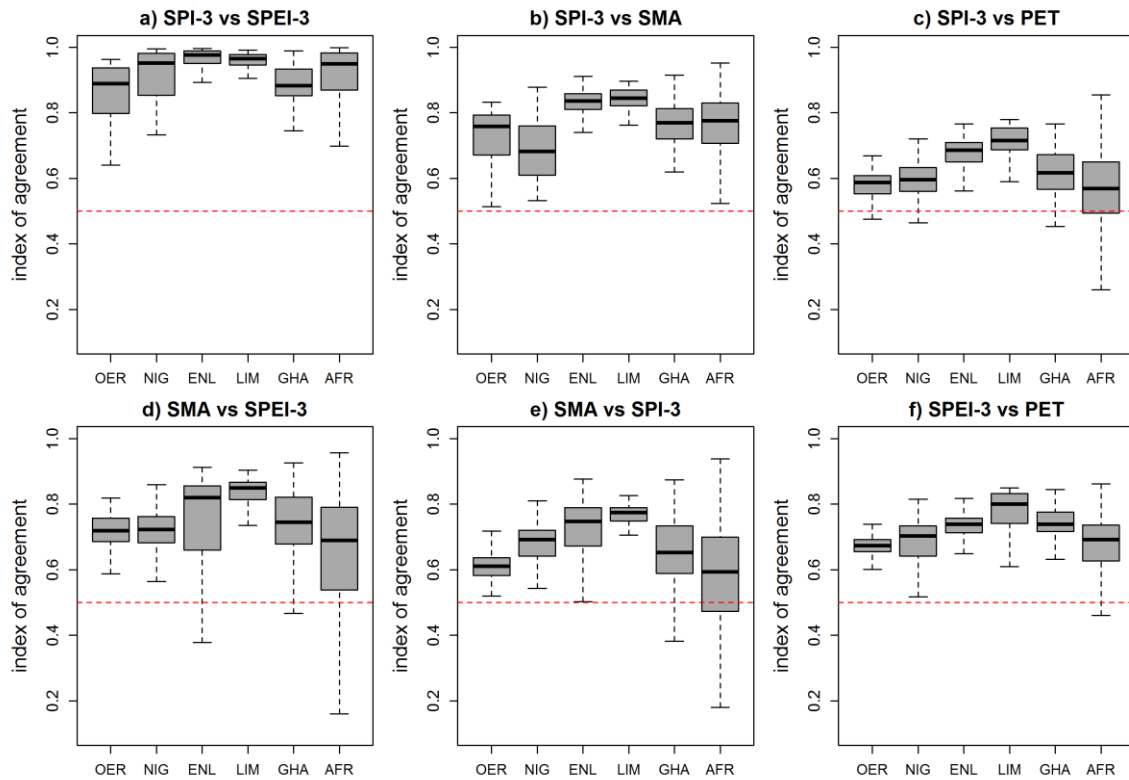
6

7

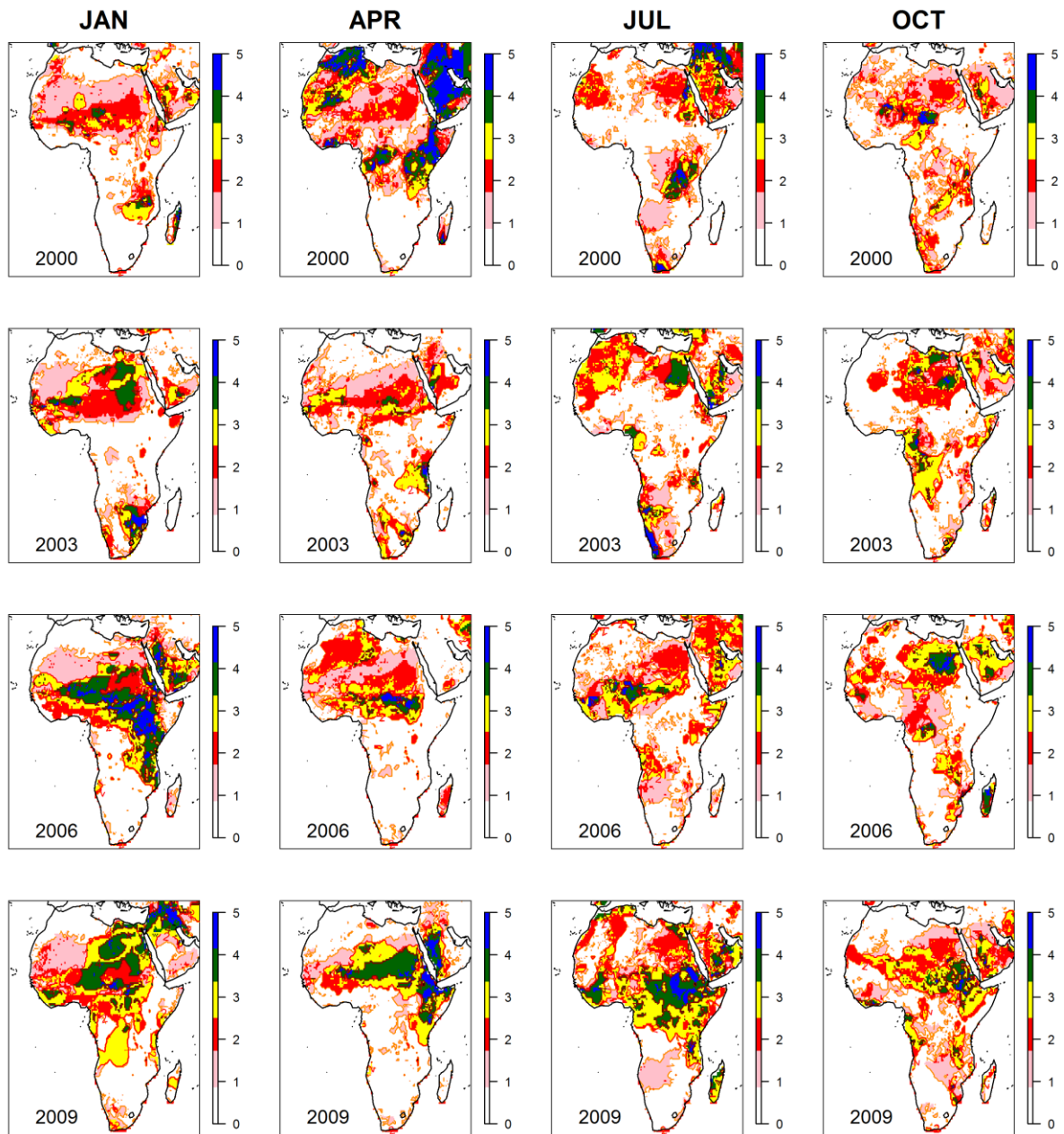
8



1 Figure 4. Monthly standardized anomalies in SPI-3 (ERA-I, GPCP, TRMM), SPEI (ERA-I  
 2 and GPCP) and Soil Moisture (SMA) for January 2000, 2003, 2006 and 2009. Solid lines  
 3 indicates the zero contour. White areas represent regions where it was not possible to compute  
 4 the gamma parameters for SPI due the large amount of zeros.  
 5



6  
 7 Figure 5. Index of agreement (d) between SPI, SPEI, SMA and PET computed using ERA-I  
 8 for the five case studies and the whole continent. (OER: Oum er-Rbia, NIG: Inner Niger  
 9 Delta, NIL: Eastern Nile, LIM: Limpopo basin and GHA: Greater Horn of Africa). Dashed  
 10 lines extend from 5th to 95th percentile of estimations, boxes extend from 25th to 75th  
 11 percentile and middle horizontal lines within each box indicate the mean for each region.  
 12  
 13  
 14  
 15  
 16  
 17



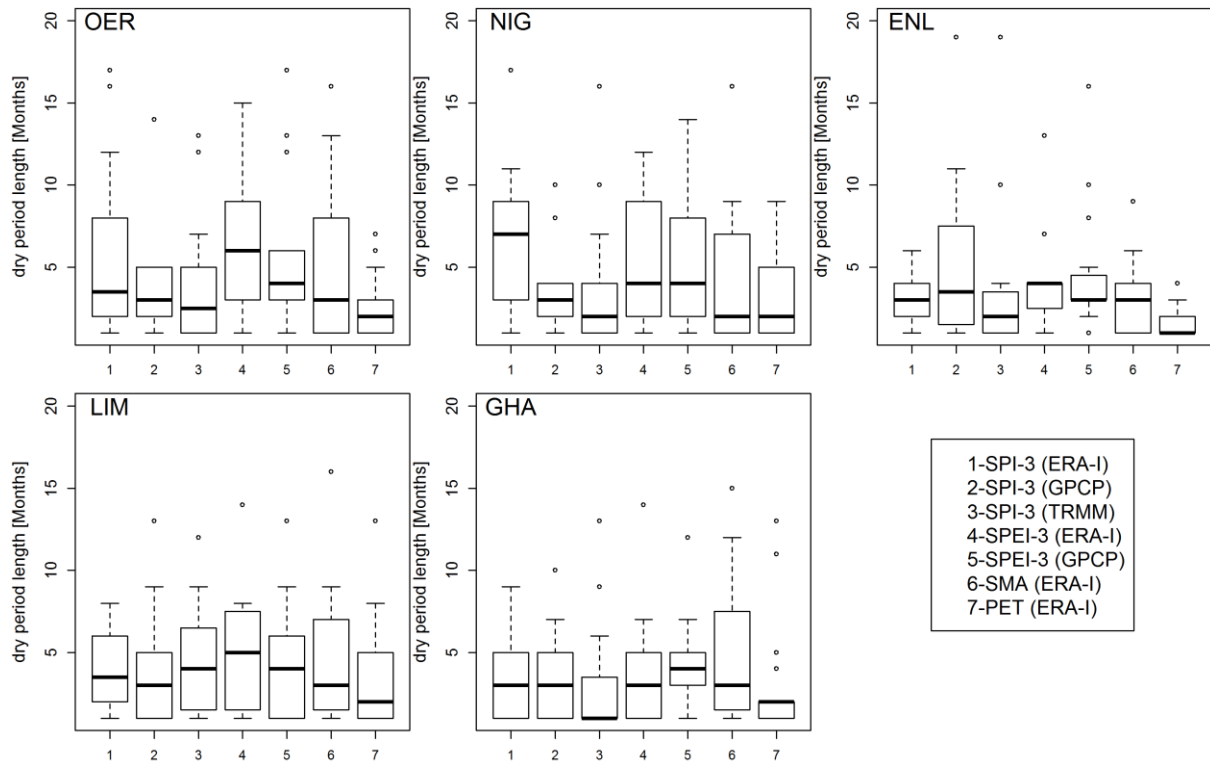
1

2 Figure 6. Month by month evolution of droughts in 2000, 2003, 2006 and 2009 according to  
 3 grid cells with SPI-3/SPEI-3 computed using ERA-I GPCP, and TRMM below -1.0. Values  
 4 are ranged between 0 (no dataset with SPI-3/SPEI-3 below the threshold) and 5 (all datasets  
 5 below threshold).

6

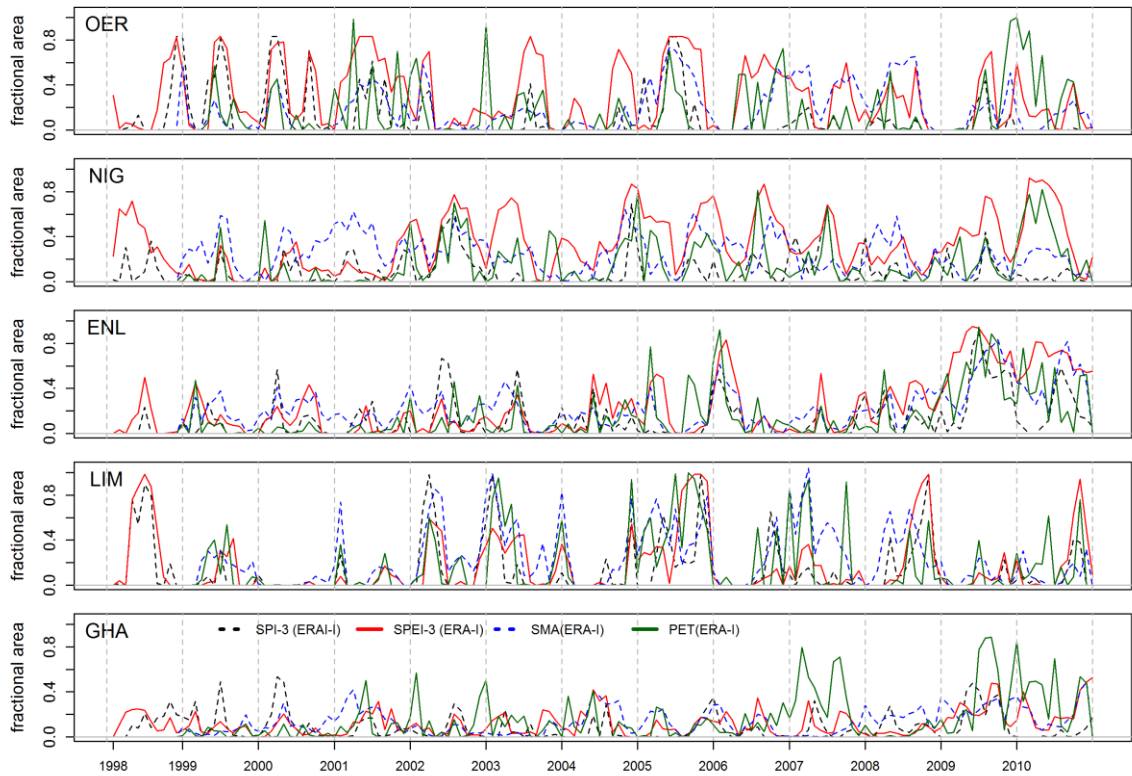
7

8



1  
 2 Figure 7. Duration of dry periods for the standardized indicators below zero in the common  
 3 period 1998-2010. (OER: Oum er-Rbia, NIG: Inner Niger Delta, NIL: Eastern Nile, LIM:  
 4 Limpopo basin and GHA: Great Horn of Africa). Dashed lines extend from 5th to 95th  
 5 percentile of estimations, boxes extend from 25th to 75th percentile and middle horizontal  
 6 lines within each box indicate the mean for each region.

7  
 8  
 9  
 10  
 11  
 12



1

2 Figure 8. Fractional area of each region under SPI, SPEI and SM and PET z-scores below -1.0  
 3 for the period 1998-2010. (OER: Oum er-Rbia, NIG: Inner Niger Delta, NIL: Eastern Nile,  
 4 LIM: Limpopo basin and GHA: Greater Horn of Africa).

5

6

7

8

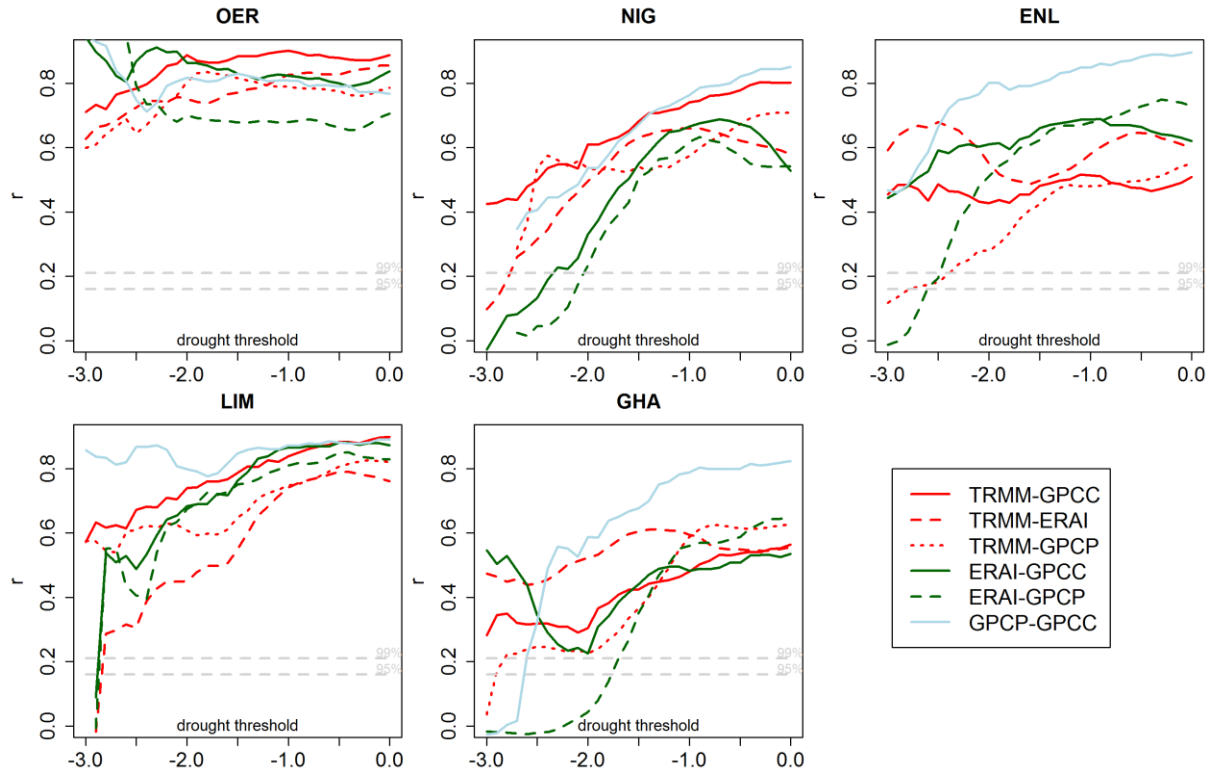
9

10

11

12





1

2 Figure 9. Correlation coefficient of fractional areas under drought between different datasets  
 3 and thresholds. The horizontal axis represents the SPI threshold below which areas are  
 4 considered to be under drought.

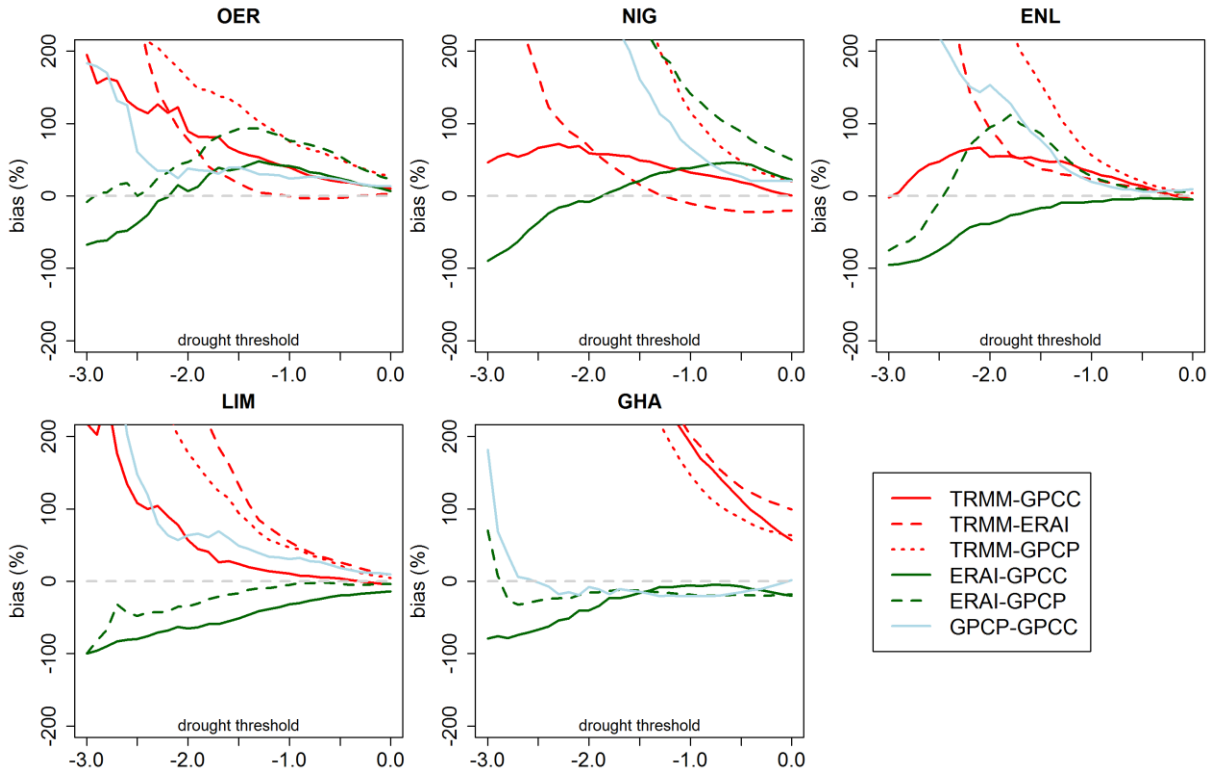
5

6

7

8

9



1

2 Figure 10. Relative bias between the estimation of fractional areas under drought for different  
 3 datasets and thresholds. The horizontal axis represents the SPI threshold below which areas  
 4 are considered to be under drought.